Preparation of AgBr Nanoparticles in Microemulsions Via Reaction of AgNO3 with CTAB Counterion

ARTICLE *in* JOURNAL OF NANOPARTICLE RESEARCH · OCTOBER 2007

Impact Factor: 2.18 · DOI: 10.1007/s11051-006-9107-4

3 AUTHORS, INCLUDING:

Maen M. Husein
The University of Calgary
50 PUBLICATIONS **587** CITATIONS
SEE PROFILE

Eva Rodil
University of Santiago de Compostela
56 PUBLICATIONS **997** CITATIONS
SEE PROFILE

Journal of Nanoparticle Research (2007) 9:787–796
DOI 10.1007/s11051-006-9107-4

Research Paper

Preparation of AgBr nanoparticles in microemulsions via reaction of $AgNO_3$ with CTAB counterion

Maen M. Husein[1,*], Eva Rodil[2,3] and Juan H. Vera[2]
[1]*Department of Chemical and Petroleum Engineering, University of Calgary, Calgary, T2N 1N4, Canada;* [2]*Department of Chemical Engineering, McGill University, Montreal, H3A 2B2, Canada;* [3]*Department of Chemical Engineering, University of Santiago de Compostela, Santiago, E-15782, Spain; *Author for correspondence (Tel.: 1-403-220-6691; E-mail: mhusein@ucalgary.ca)*

Received 24 October 2005; accepted in revised form 3 April 2006

Key words: nanoparticles, microemulsions, photosensitive, quantum dots, surfactant, counterion, CTAB

Abstract

Nanoparticles of AgBr were prepared by precipitating AgBr in the water pools of microemulsions consisting of CTAB, *n*-butanol, isooctane and water. An aqueous solution of $AgNO_3$ added to the microemulsion was the source of Ag^+ ions. The formation of AgBr nanoparticles in microemulsions through direct reaction with the surfactant counterion is a novel approach aimed at decreasing the role of intermicellar nucleation on nanoparticle formation for rapid reactions. The availability of the surfactant counterion in every reverse micelle and the rapidity of the reaction with the counterion trigger nucleation within individual reverse micelles. The effect of the following variables on the particle size and size distribution was investigated: the surfactant and cosurfactant concentrations, moles of $AgNO_3$ added, and water to surfactant mole ratio, *R*. High concentration of the surfactant or cosurfactant, or high water content of the microemulsion favored intermicellar nucleation and resulted in the formation of large particles with broad size distribution, while high amounts of $AgNO_3$ favored nucleation within individual micelles and resulted in small nanoparticles with narrow size distribution. A blue shift in the UV absorption threshold corresponding to a decrease in the particle size was generally observed. Notably, the variation of the absorption peak size with the nanoparticle size was opposite to those reported by us in previous studies using different surfactants.

Introduction

Silver bromide is used for high-speed photographic materials, X-ray films and instant photography (Sugimoto & Shiba, 2000). The sensitivity of photographic materials is dependant on their grain size and crystal structure, and improves as the grain size decreases (Belloni et al., 1991; Zhang & Mostafavi, 1997). Nanoparticles of silver bromide have also attracted attention as a model material to study the quantum confinement effects of indirect gap semiconductors (Johansson et al., 1992; Chen et al., 1994; Zhang & Mostafavi, 1997). More recently, silver bromide supported on silica was used as a photocatalyst for hydrogen generation from a solution of methanol and water (Kakuta et al., 1999). Interfacial reaction rates per gram of catalyst increase significantly as the size of the catalyst particles decreases.

Water-in-oil microemulsions, or reverse micelles, serve as suitable reaction medium for the preparation of a wide variety of nanoparticles. This is due to

their ability to solubilize reactants in their nanosize reactor water pools, and to stabilize the resulting nanoparticle by the protective surfactant layer. Most of the work on nanoparticle formation using microemulsions employed mixing of two identical microemulsions each solubilizes one of the reactants forming the particles in its water pools (Monnoyer et al., 1995; Pillai et al., 1995; Bagwe & Khilar, 1997). Upon mixing the two microemulsions, reverse micelles containing the different reactants diffuse, collide, their surfactant layer opens allowing the two reactants to mix and the reaction to take place. For rapid reactions, the surfactant surface layer opening is the rate determining step (Bommarius et al., 1990). A rigid surfactant surface layer tends to resist opening, thus slowing down the reaction and causing simultaneous nucleation and growth. This, in turn, results in the formation of large nanoparticles with broad size distribution (Chew et al., 1990).

In previous studies, we have presented a novel method for the preparation of precipitates of nanoparticles in microemulsions aimed at minimizing the impact of the surfactant surface layer opening on nanoparticle formation for rapid reactions (Husein et al., 2003, 2004). The method is based on a direct reaction of an added salt solution with the surfactant counterion while incorporating the salt solution into the reverse micelles. Reactions with surfactant counterions are characterized by rapid kinetics, due to the compartmentalization effect (Husein et al., 2001), and the availability of, at least, one of the reactants in each reverse micelle. Combined together, these two factors contribute towards nuclei formation within individual reverse micelles. Nucleation takes place within reverse micelles containing monomer concentration that exceeds the minimum nucleation concentration. Hence, nucleation becomes less dependant on the intermicellar exchange of solubilizate and the surfactant surface layer opening. Our previous studies involved the formation of silver chloride and silver bromide nanoparticles through addition of aqueous solutions of $AgNO_3$ to microemulsions formed with dioctyldimethylammonium chloride and bromide, respectively. In the current study, we present the formation of AgBr in single microemulsions formed with hexadecyltrimethylammonium bromide, CTAB. Microemulsions formed with CTAB are favored as reaction media since they allow for high reactant loading. Water-in-oil microemulsions of CTAB form stable microemulsions at high water to surfactant mole ratios and high salt concentrations (Fang & Yang, 1999).

Experimental work

The microemulsions were prepared by mixing certain amounts of hexadecyltrimethylammonium bromide, CTAB 99% pure (Sigma, Oakville, ON), *n*-butanol, 99.4% pure (Fisher Scientific, Montreal, QC), isooctane, 99% pure (Fisher Scientific, Montreal, QC) and deionized water in a volumetric flask until a clear phase was obtained. A specified volume of 12% (w/v) $AgNO_3$ aqueous solution (A&C, Montreal, QC) was added to a 15 ml volume of the microemulsion to achieve the required moles of $AgNO_3$ and water to surfactant mole ratio. Upon addition of $AgNO_3$, the solution turned to milky yellow. A clear solution was obtained after mixing for 3 min in a vortex mixer and then placing the solution for 10 min in an ultrasonic bath. The sample was then left to stand at room temperature for 12 h. The UV absorption of the colloidal AgBr nanoparticles was measured using Cary Varian 1/3 UV/visible spectrophotometer (Varian Techtron Pty Ltd., Victoria, Australia). A range of wavelengths between 190 and 500 nm was covered. Reference solutions of microemulsions identical to the ones used to prepare the experimental samples were used for the UV measurements.

The AgBr nanoparticles were collected for particle size analysis by adding thiophenol capping agent (Aldrich, Milwaukee, WI); 10 μl thiophenol/1 ml microemulsion. The sample was vigorously mixed for 1 min, placed in an ultrasonic bath for 1 h and left to stand at room temperature for 24 h. This treatment resulted in the formation of a yellow precipitate of thiophenol–AgBr. It should be noted that the addition of the capping agent to a nanoparticle-free microemulsion did not result in any precipitation or any observable change in the microemulsion. The sample was then centrifuged for 5 min at 1000 rpm to separate the precipitate. A 10 ml of methanol, 99.8% pure (Fisher Scientific, Montreal, QC) was added to the precipitate followed by vigorous mixing for 2 min. The methanol system was placed in the ultrasonic bath for 2 h. One drop of the resulting suspension was

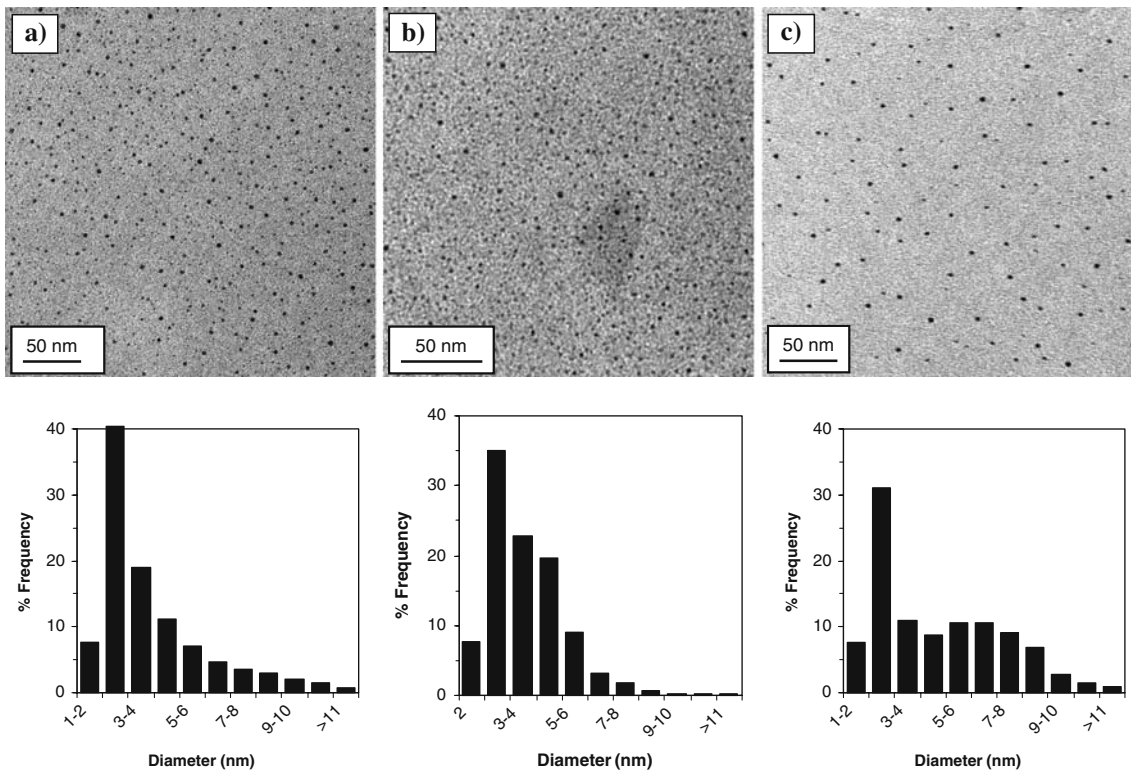

Figure 1. TEM photographs and the corresponding particle size distribution histograms for 1.6 M *n*-butanol, n_{AgNO_3} = 0.07 mmol, $R = 9$, and different concentrations of CTAB. (a) 0.1 M; (b) 0.2 M; (c) 0.3 M.

placed on a copper grid covered with Formvar, and left to evaporate for 24 h. In order to minimize possible coagulation during evaporation, the copper grid was manually shaken for few seconds to ensure that only a thin layer of the methanol suspension remains on the grid. Photographs of the nanoparticles were taken at different degrees of magnification from different locations on the grid using a JEOL 2000FX Transmission Electron Microscope, TEM (JEOL USA Inc., MA), equipped with a Gatan 792 Bioscan 1k×1k wide angle multiscan CCD camera. Histograms showing the particle size distribution were constructed based on the different photographs. An average of 2500 particles was used per histogram.

Results and discussion

Incorporating the added salt

Upon addition of the $AgNO_3$ aqueous solution, the microemulsion turned milky yellow. The turbidity disappeared after mixing indicating a complete incorporation of the $AgNO_3$ solution and the AgBr precipitate into the microemulsion water pools. It is believed that most of the AgBr precipitate formed after incorporating the $AgNO_3$ solution into the water pools by virtue of the large surface the microemulsion provides for the reaction. Similar observations were reported in our previous studies (Husein et al., 2003, 2004).

Effect of CTAB concentration

The effect of increasing the concentration of CTAB from 0.1 to 0.3 M, at constant moles of $AgNO_3$, n_{AgNO_3}, of 0.07 mmol, constant concentration of *n*-butanol of 1.6 M and constant water-to-surfactant mole ratio, *R*, of 9 is depicted in Figures 1a–c and 2. Figure 1a–c show typical TEM photographs and the corresponding particle size distribution histograms, and Figure 2 shows the UV absorption of the colloidal AgBr nanoparticles.

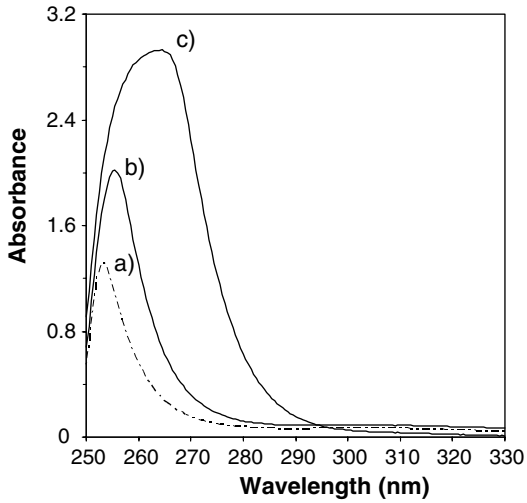

Figure 2. Absorption spectra of the colloidal AgBr nanoparticles for 1.6 M *n*-butanol, n_{AgNO_3} = 0.070 mmol, $R = 9$, and different concentrations of CTAB. (a) 0.1 M; (b) 0.2 M; (c) 0.3 M. Reference cell: 1.6 M *n*-butanol, $R = 9$, (a) 0.1 M; (b) 0.2 M; (c) 0.3 M CTAB.

The TEM results indicate that the nanoparticle size increased and the particle size distribution became broader as CTAB concentration increased. These trends agree with our previous results (Husein et al., 2003, 2004). The increase in the particle size and the particle size distribution in response to increasing the surfactant concentration suggest a growth process which took place on a smaller number of nuclei and proceeded in parallel to nucleation. This is a characteristic of intermicellar nucleation governed by slow surfactant surface layer opening. Higher surfactant concentration, at fixed values of all other variables, contributes towards increasing the number of reverse micelles (Fang & Yang, 1999). Larger number of reverse micelles reduces the Ag^+ ion occupancy number, i.e. the number of Ag^+ ions per reverse micelle. Consequently, once incorporating the $AgNO_3$ solution, the number of reverse micelles containing AgBr monomers with concentration exceeding the critical nucleation concentration drops. Nucleation becomes mainly dependent on intermicellar exchange of solubilizate, which for rigid surfactant layer results in the formation of larger particles with broader size distribution.

Figure 2 shows that the UV absorption of the colloidal AgBr nanoparticles occurred in a range of wavelengths between 250 and 290 nm. Similar absorption range was reported for colloidal AgBr nanoparticles obtained using the mixing of two microemulsions method (Correa et al., 2000; Zhang et al., 2000; Husein et al., 2004). No UV peaks were detected in the 400 nm region, suggesting that the reduction of Ag^+ to Ag as a result of exposure to light was limited (Kakuta et al., 1999; Husein et al., 2004). Figure 2 portrays a red shift in the absorption threshold associated with the increase in the mean nanoparticle size. This trend had been reported by other researchers (Weller et al., 1986; Towey et al., 1990; Bagwe & Khilar, 2000). The shift in the absorption threshold was not pronounced for the silver halide nanoparticles prepared in microemulsions of dioctyldimethylammonium chloride and bromide (Husein et al., 2003; 2004). Instead, these systems depicted an increase in the absorption peak accompanying a decrease in the particle size. The increase in the peak size with the decrease in the particle size was also inferred from other studies in the literature (Hirai et al., 1993, 1994; Vossmeyer et al., 1994; Bagwe & Khilar, 2000). In the current work, however, a decrease in the peak size accompanied the decrease in the particle size. This result was confirmed by repeating the experiments several times. In addition to the particle size and concentration, the size and location of the UV absorption peaks and shoulders are function of excess lattice ion, surfactant species and surfactant concentration (Tanaka et al., 1979). Since the potential excess lattice ion, Br^-, was also present in our previous study (Husein et al., 2004), it is concluded that a possible interaction between CTAB and AgBr nanoparticles might have resulted in this opposite trend. This hypothesis was tested by studying the effect of reducing the interaction between the CTAB layer and the AgBr nanoparticles upon increasing the water to surfactant mole ratio, *R*.

Effect of water to surfactant mole ratio, R

The amount of water in w/o microemulsions dictates the degree of interaction between the surfactant head groups and the nanoparticles, and the rigidity of the surfactant protective layer. Less interaction between the surfactant head groups and the nanoparticles and less surface rigidity induces nanoparticle aggregation. The effect of the water content was studied by increasing *R* from 9

to 29 at n_{AgNO_3} = 0.070 mmol, and concentrations of CTAB and *n*-butanol of 0.2 and 1.6 M, respectively. The results are shown in Figure 3a–c as typical TEM photographs and the corresponding particle size distribution histograms, and in Figure 4 as the UV absorption of the colloidal AgBr nanoparticles.

The TEM photographs and the particle size distribution histograms show a dramatic increase in the particle size and the particle size distribution as *R* increased. The increase in the particle size and the particle size distribution is attributed to slow nucleation accompanied by particle growth and aggregation. Increasing the water content of the microemulsion at constant values of all the other variables promotes intermicellar nucleation in the following manner. High water content introduces a dilution effect and reduces nucleation within individual reverse micelles as a result of decreasing the Ag^+ ion occupancy number. Hence, nucleation becomes dependant on the intermicellar exchange of solubilizate. In addition, high water content reduces the rigidity of the surfactant protective layer. Less rigid surface has two opposite effects on the particle size and particle size distribution. On one hand, less rigid surface increases the rate of nucleation, which in turn, provides more seeds for growth and results in smaller particles (Chew et al., 1990). This factor might have been, however, overshadowed by the reduction in the rate of nucleation associated with the dilution effect. On the other hand, less rigid surface promotes particle aggregation as a result of reducing the interaction between the surfactant head group and the particles (Chew et al., 1990), and subsequently larger particles with larger size distribution form.

Figure 4 shows no significant shift in the UV absorption threshold. The UV absorption peaks in Figure 4 are smaller for larger nanoparticle size. This trend is consistent with the one obtained in our previous studies (Husein et al., 2003, 2004), and supports the hypothesis that the larger absorption peaks associated with the larger nanoparticles obtained in the effect of CTAB

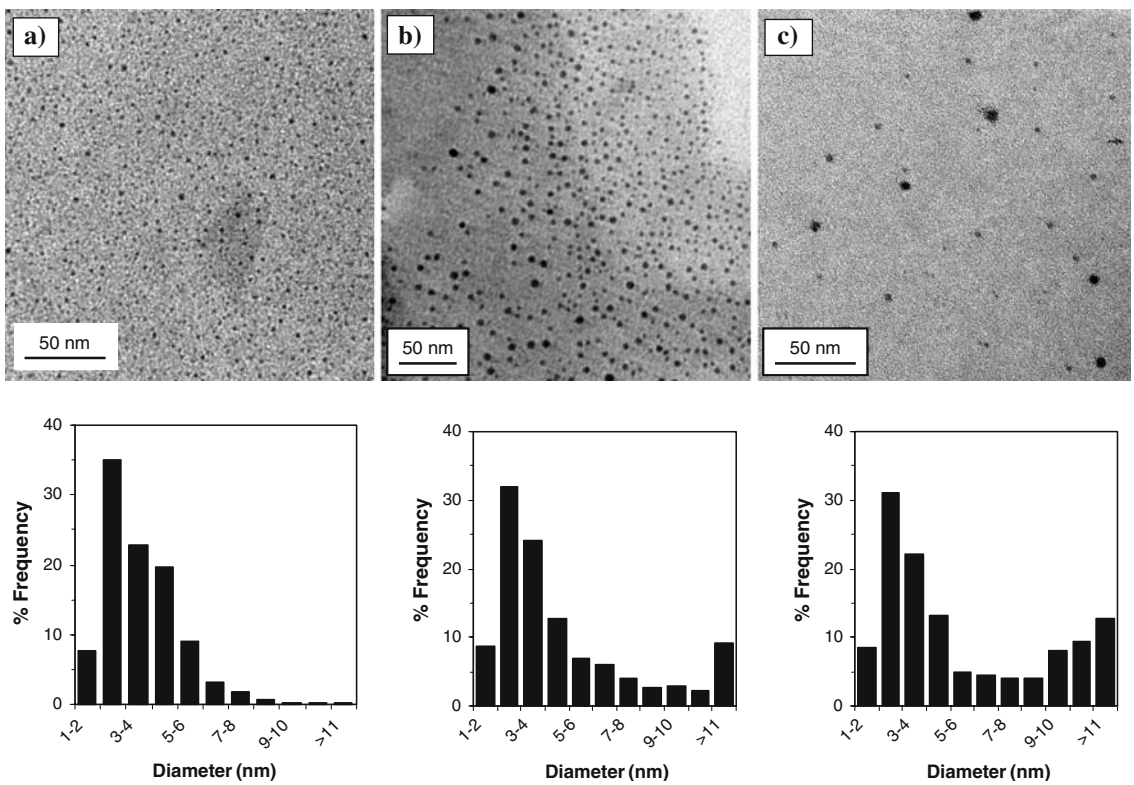

Figure 3. TEM photographs and the corresponding particle size distribution histograms for 0.2 M CTAB, 1.6 M *n*-butanol, n_{AgNO_3} = 0.070 mmol, and different values of *R*. (a) 9; (b) 20; (c) 29.

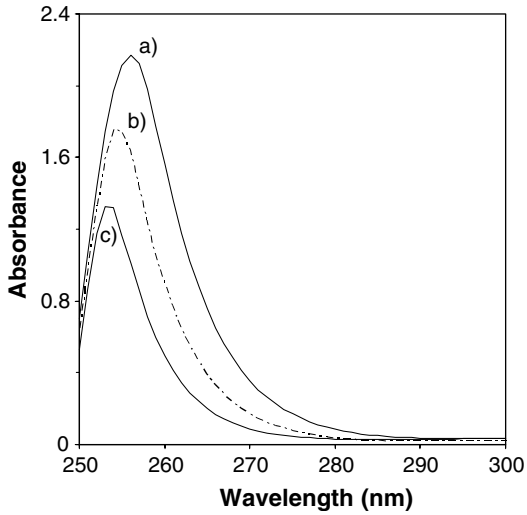

Figure 4. Absorption spectra of the colloidal AgBr nanoparticles for 0.2 M CTAB, 1.6 M *n*-butanol, n_{AgNO_3} = 0.070 mmol, and different values of *R*. (a) 9; (b) 20; (c) 29. Reference cell: 0.2 M CTAB, 1.6 M *n*-butanol, (a) 9; (b) 20; (c) 29 *R*.

experiment might have resulted from an interaction between the surfactant head groups and the nanoparticles.

Effect of moles of $AgNO_3$, n_{AgNO_3}

The TEM photographs and the corresponding particle size distribution histograms which capture the effect of increasing the number of moles of $AgNO_3$, n_{AgNO_3}, are shown in Figure 5a–c. The UV absorption of the colloidal AgBr nanoparticles is shown in Figure 6. The number of moles of $AgNO_3$ was increased from 0.035 to 0.07 mmol at constant CTAB and *n*-butanol concentrations of 0.2 and 1.6 M, respectively, and a constant *R* of 9.

Figure 5a–c show a decrease in the particle size as n_{AgNO_3} increased. This decrease in the particle size is captured by the blue shift in the absorption threshold of the UV spectra in Figure 6. Smaller particle size suggests particle growth commencing on larger number of nuclei. Increasing the number

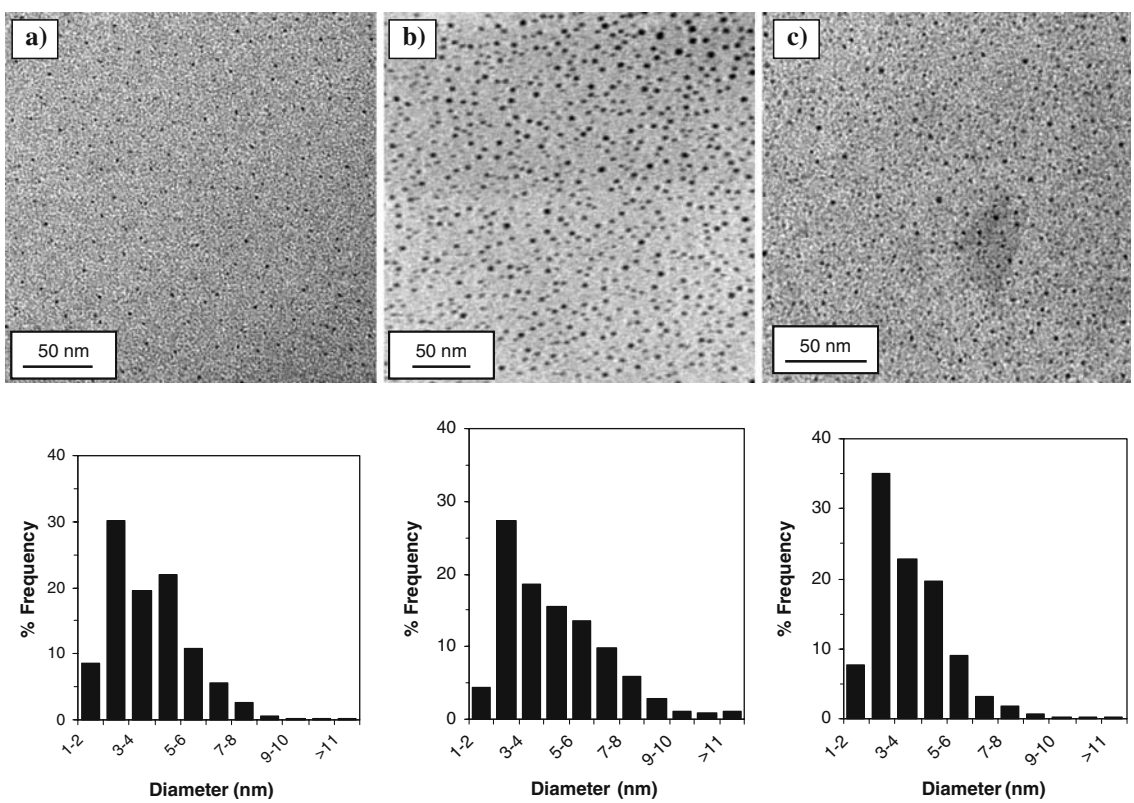

Figure 5. TEM photographs and the corresponding particle size distribution histograms for 0.2 M CTAB, 1.6 M *n*-butanol, $R = 9$, and different moles of $AgNO_3$, n_{AgNO_3}. (a) 0.035 mmol; (b) 0.053 mmol; (c) 0.070 mmol.

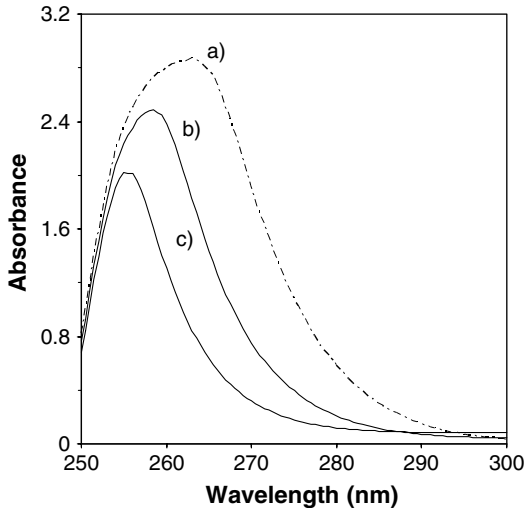

Figure 6. Absorption spectra of the colloidal AgBr nanoparticles for 0.2 M CTAB, 1.6 M *n*-butanol, $R = 9$, and different moles of $AgNO_3$, n_{AgNO_3}. (a) 0.035 mmol; (b) 0.053 mmol; (c) 0.070 mmol. Reference cell: 0.2 M CTAB, 1.6 M *n*-butanol, $R = 9$.

of moles of $AgNO_3$, at constant values of the other variables, increases Ag^+ ion occupancy number and breeds more reverse micelles with AgBr monomer concentration exceeding the minimum nucleation concentration. Consequently, nucleation proceeds primarily within individual reverse micelles and intermicellar exchange of solubilizate contributes to the growth process. Combined together these factors result in the formation of smaller particles with narrower size distribution.

Figure 6 shows that the peak size decreased as the nanoparticle size decreased. This trend agrees with the trend pertaining to the effect of CTAB experiment. Smaller particle size allows for more interaction with CTAB molecules.

Effect of n-butanol concentration

The main role of the cosurfactant is to stabilize a microemulsion system by participating at the water/oil interface and screening the repulsion forces among the surfactant head groups (Wang et al., 1994). A stable microemulsion provides a rigid surfactant layer which protects its nanoparticle content from aggregation. A rigid surfactant layer, on the other hand, slows down nucleation and promotes simultaneous growth when nucleation is governed by the intermicellar exchange of solubilizate (Chew et al., 1990; Bagwe & Khilar, 1997). In this experiment the concentration of *n*-butanol was increased from 1.6 to 3.5 M at CTAB concentration of 0.2 M, n_{AgNO_3} of 0.070 mmol and R of 9. The resulting TEM photographs and the corresponding particle size distribution histograms are given in Figure 7a–c, and the UV absorption of the colloidal nanoparticles is given in Figure 8.

The TEM results show a slight decrease followed by a slight increase in the particle size as *n*-butanol concentration increased. This trend can be explained as follows. By screening the repulsion forces among the surfactant head groups, the cosurfactant increases the compactness of molecules at the interface, and subsequently the curvature and the rigidity of the surfactant layer increase (Wang et al., 1994; Curri et al., 2000). Rigid surfactant layer resists opening upon collision of reverse micelles, slows down intermicellar nucleation and prevents aggregation of the resulting nanoparticles. If Ag^+ ion occupancy number is high enough, nucleation proceeds within individual reverse micelles once accommodating the $AgNO_3$ solution, and intermicellar exchange of solubilizate contributes to the growth process. Consequently, smaller size nanoparticles with narrower size distribution form. Very high concentration of the cosurfactant, on the other hand, increases the polarity of the oil phase and makes it more accommodating to the non-dissociated surfactant molecules (Curri et al., 2000). Lower population of surfactant molecules in the surfactant protective layer promotes simultaneous nucleation and growth, in addition to aggregation of the nanoparticles.

Figure 8 shows no shift in the absorption threshold and a general decrease in the size of the UV absorption peaks as *n*-butanol concentration increased. This decrease was not as pronounce as that caused by the other variables considered in this study, since the particle size did not vary much with *n*-butanol concentration.

Conclusions

Silver bromide nanoparticles were prepared by addition of measured volumes of $AgNO_3$ aqueous solution to w/o microemulsions consisting of CTAB, *n*-butanol and water in isooctane. The vol-

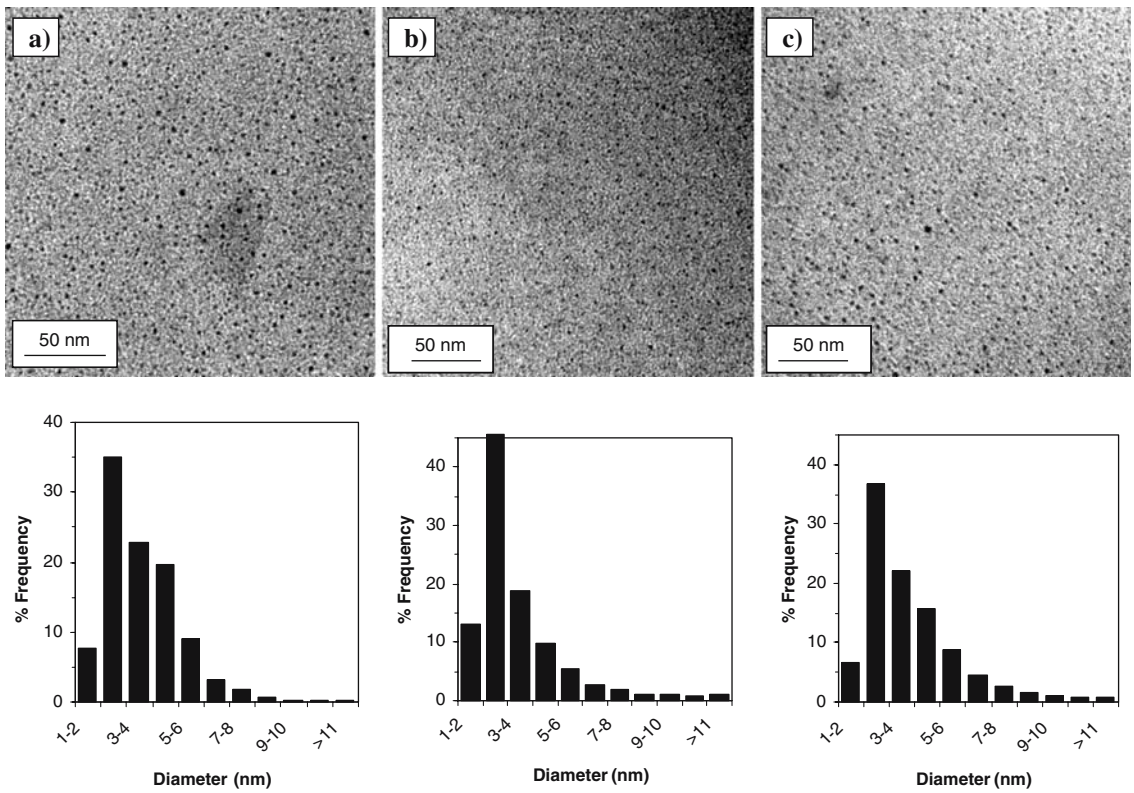

Figure 7. TEM photographs and the corresponding particle size distribution histograms for 0.2 M CTAB, n_{AgNO_3} = 0.070 mmol, $R = 9$, and different concentrations of *n*-butanol. (a) 1.6 M; (b) 2.5 M; (c) 3.5 M.

ume of $AgNO_3$ solution was in the range that could be incorporated in the system without causing collapse of the microemulsion. The precipitate of AgBr nanoparticles formed in the water pools of the microemulsion as a result of a reaction between Ag^+ and the Br^- counterion. The formation of nanoparticles in w/o microemulsion through direct reaction with the surfactant counterion is a novel approach aimed at promoting precipitation within individual micelles. This method decreases the role of surfactant layer opening and intermicellar exchange of solubilizate on the particle size distribution for rapid reactions. When the concentration of Ag^+ ion was high enough, nucleation within individual reverse micelles commenced once incorporating the $AgNO_3$ solution, and nucleation became less dependent of the intermicellar exchange of solubilizate. The reaction occurs almost instantly within individual reverse micelles by virtue of the very rapid nature of reactions with the surfactant counterion, and the existence of the counterion in every reverse micelle. For fast reactions, such as precipitation reactions, intermicellar nucleation is limited by the surfactant surface layer opening. Slow surfactant layer opening limits the number of nuclei and promotes simultaneous growth, which results in the formation of large particles with broad size distribution. Small particles with narrow size distribution formed in response to the variables that increased the Ag^+ ion occupancy number once incorporating the $AgNO_3$ solution added to the microemulsions. The amount of $AgNO_3$ added was the only variable in this study that promoted nucleation within individual reverse micelles. Increasing the CTAB concentration and the water to surfactant mole ratio, R, resulted in a dilution effect, which limited nucleation within individual reverse micelles, and a nucleation process governed by the intermicellar exchange of solubilizate. Aggregation, which also results in the formation of large particles with broad size distribution, was induced by variables which decreased the interac-

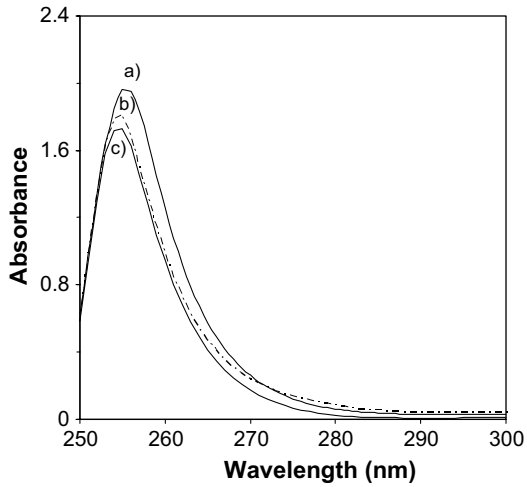

Figure 8. Absorption spectra of the colloidal AgBr nanoparticles for 0.2 M CTAB, n_{AgNO_3} = 0.070 mmol, $R = 9$, and different concentrations of *n*-butanol. (a) 1.6 M; (b) 2.5 M; (c) 3.5 M. Reference cell: 0.2 M CTAB, $R = 9$, (a) 1.6 M; (b) 2.5 M; (c) 3.5 M *n*-butanol.

tion between the surfactant protective layer and the nanoparticles; including increasing R value and high *n*-butanol concentration.

A red shift in the UV absorption threshold was associated with larger nanoparticles. The size of the absorption peak, however, decreased as the nanoparticle size decreased. This trend is attributed to an interaction between the surfactant head groups and the nanoparticles.

Acknowledgements

The authors thank the Natural Sciences and Engineering Research Council of Canada and the Ministerio de Ciencia y Tecnologia of Spain (project 2004/PC059) for their financial support.

References

Bagwe R.P. & K.C. Khilar, 1997. Effects of intermicellar exchange rate and cations on the size of silver chloride nanoparticles formed in reverse micelles of AOT. Langmuir 13, 6432–6432.

Bagwe R.P. & K.C. Khilar, 2000. Effects of intermicellar exchange rate on the formation of silver nanoparticles in reverse microemulsions of AOT. Langmuir 16, 905–910.

Belloni J., M. Mostafavi, J. Marignier & J. Amblard, 1991. Quantum size effects and photographic development. J. Imaging Sci. 35, 68–74.

Bommarius A.S., J.F. Holzwarth, D.I. Wang & A.T. Hatton, 1990. Coalescence and solubilizate exchange in a cationic four-component reversed micellar system. J. Phys. Chem. 94, 7232–7339.

Chen W., G. McLendon, A. Marchetti, J.M. Rehm, M.I. Freedhoff & C. Myers, 1994. Size dependence of radiative rates in the indirect band gap material AgBr. J. Am. Chem. Soc. 116, 1585–1586.

Chew C.H., L.M. Gan & D.O. Shah, 1990. The effect of alkanes on the formatin of ultrafine silver bromide particles in ionic w/o microemulsions. J. Dispersion Sci. Technol. 11, 593–609.

Correa N.M., H. Zhang & Z.A. Schelly, 2000. Preparation of AgBr quantum dots via electroporation of vesicles. J. Am. Chem. Soc. 122, 6432–6434.

Curri M.L., A. Agostiano, L. Manna, M.D. Monica, M. Catalano, L. Chiavarone, V. Spagnolo & M. Lugara, 2000. Synthesis and characterization of CdS nanoclusters in a quaternary microemulsion: the role of the cosurfactant. J. Phys. Chem. B 104, 8391–8397.

Fang X. & C.J. Yang, 1999. An experimental study on the ralationship between the physical properties of CTAB/Hexanol/Water reverse micelles and ZrO_2-Y_2O_3 nanoparticles prepared. Colloid Interface Sci. 212, 242–251.

Hirai T., H. Sato & I. Komasawa, 1993. Mechanism of formation of titanium dioxide ultrafine particles in reverse micelles by hydrolysis of titanium tetrabutoxide. Ind. Eng. Chem. Res. 32, 3014–3019.

Hirai T., H. Sato & I. Komasawa, 1994. Mechanism of formation of CdS and ZnS ultrafine particles in reverse micelles. Ind. Eng. Chem. Res. 33, 3262–3266.

Husein M.M., E. Rodil & J.H. Vera, 2003. Formation of silver chloride nanoparticles in microemulsions by direct precipitation with the surfactant counterion. Langmuir 19, 8467–8474.

Husein M.M., E. Rodil & J.H. Vera, 2004. Formation of silver bromide precipitate of nanoparticles in a single microemulsion utilizing the surfactant counterion. J. Colloid Interface Sci. 273, 426–434.

Husein M.M., M. Weber & J.H. Vera, 2001. Nucleophilic substitution sulfonation in emulsions: formation of sodium benzyl sulfonate. Can. J. Chem. Eng. 79, 744–750.

Johansson K., A. Marchetti & G. McLendon, 1992. Effect of size restriction on the static and dynamic emission behavior of silver bromide. J. Phys. Chem. 96, 2873–2879.

Kakuta N., N. Goto, H. Ohkita & T. Mizushima, 1999. Silver bromide as a photocatalyst for hydrogen generation from CH_3OH/H_2O solution. J. Phys. Chem. B 103, 5917–5919.

Monnoyer Ph., A. Fonseca & J. Nagy, 1995. Preparation of colloidal AgBr particles from microemulsions. Colloids Surf. A 100, 233–243.

Pillai V., P. Kumar, M. Hou, P. Ayyub & D. Shah, 1995. Preparation of nanoparticles of silver halides, Superconductors and magnetic materials using water-in-oil microemulsions as nano-reactors. Adv. Colloid Interface Sci. 55, 241–269.

Sugimoto T. & F. Shiba, 2000. Spontaneous nucleation of monodisperse silver halide particles from homogeneous gelatin solution II: silver bromide. Colloids Surf. A 164, 205–215.

Tanaka T., H. Saijo & T. Matsubara, 1979. Optical absorption studies of the growth of microcrystals in nascent silver iodide hydrosols. J. Photogr. Sci. 27, 60–65.

Towey T.F., A. Khan-Lodhi & B.H. Robinson, 1990. Kinetics and mechanism of formation of quantum-sized cadmium sulphide particles in water-aerosol-OT-oil microemulsions. J. Chem. Soc. Faraday Trans. 86, 3757–3762.

Vossmeyer T., L. Katsikas, M. Giersig, I. Popovic, K. Diesner & A. Chemseddine, 1994. Characterization, size dependent oscillator strength, temperature shift of the excitonic transition energy, and reversible absorbance shift. J. Phys. Chem. 98, 7665–7673.

Wang W., M.E. Weber & J.H. Vera, 1994. Effect of alcohol and salt on water uptake of reverse micelles formed by dioctyldimethylammonium chloride (DODMAC) in isooctane. J. Colloid Interface Sci. 168, 422–427.

Weller H., H.M. Schmidt, U. Koch, A. Fojtik, S. Baral, A. Henglein, W. Kunath, K. Weiss & E. Dieman, 1986. Photochemistry of colloidal semiconductors onset of light absorption as a function of size of extremely small CdS particles. Chem. Phys. Lett. 124, 557–560.

Zhang H. & M. Mostafavi, 1997. UV-absorption observation of the silver bromide growth from a single molecule to the crystal in solution. J. Phys. Chem. B 101, 8443–8448.

Zhang H., Z.A. Schelly & D.S. Marynick, 2000. Theoretical study of the molecular and electronic structures of neutral silver bromide clusters (AgBr)n, n = 1–9. J. Phys. Chem. A 104, 6287–6294.